

Generalization and Representational Limits of Graph Neural Networks

Vikas K. Garg

Stefanie Jegelka

Tommi Jaakkola

CSAIL, MIT

Abstract

We address two fundamental questions about graph neural networks (GNNs). First, we prove that several important graph properties cannot be computed by GNNs that rely entirely on local information. Such GNNs include the standard message passing models, and more powerful spatial variants that exploit local graph structure (e.g., via relative orientation of messages, or local port ordering) to distinguish neighbors of each node. Our treatment includes a novel graph-theoretic formalism. Second, we provide the first data dependent generalization bounds for message passing GNNs. This analysis explicitly accounts for the local permutation invariance of GNNs. Our bounds are much tighter than existing VC-dimension based guarantees for GNNs, and are comparable to Rademacher bounds for recurrent neural networks.

1 Introduction

Graph neural networks (Scarselli et al., 2009; Gori et al., 2005), in their various incarnations, have emerged as models of choice for embedding graph-structured data from a diverse set of domains, including molecular structures, knowledge graphs, biological networks, social networks, and n -body problems (Duvenaud et al., 2015; Defferrard et al., 2016; Battaglia et al., 2016; Zhang et al., 2018b; Santoro et al., 2018; Yun et al., 2019; Jin et al., 2019).

The working of a graph neural network (GNN) on an input graph, with a feature vector associated with each node, can be outlined as follows. Layer ℓ of the GNN updates the embedding of each node v by aggregating the feature vectors, or node and/or edge embeddings, of v 's neighbors from layer $\ell - 1$ via a non-linear transformation, possibly combining this with v 's embedding. The exact form of aggregate and combine steps varies across architectures, and empirical success has been demonstrated for several variants. These include Graph Convolutional Network (GCN) by Kipf and Welling (2017), Graph Attention Network (GAT) by Veličković et al. (2018), Graph Isomorphism Network (GIN) by Xu et al. (2019), and GraphSAGE by Hamilton et al. (2017). GNNs are known to have fundamental connections to message passing (Dai et al., 2016; Gilmer et al., 2017), the Weisfeiler-Lehman (WL) graph isomorphism test (Xu et al., 2019; Morris et al., 2019), and local algorithms (Sato et al., 2019; Loukas, 2020).

In this work, we investigate the representational limitations and generalization properties of GNNs. That is, we examine the performance of GNNs from a learning perspective: (a) how well they can discriminate graphs that differ in a specified graph property (represented by assigning different labels to such graphs), and (b) how well they can predict labels, e.g., a graph property, for unseen graphs. Specifically, we focus on classification: (1) a GNN with learnable parameters embeds the nodes of each input graph, (2) the node embeddings are combined into a single graph vector via a *readout* function such as sum, average, or element-wise maximum, and (3) a parameterized classifier makes a binary prediction on the resulting graph vector.

Our contributions. (1) First, we show that there exist simple graphs that cannot be distinguished by GNNs that generate node embeddings solely based on local information. As a result, these GNNs cannot compute important graph properties such as longest or shortest cycle, diameter, or clique information. This limitation holds for popular models such as GraphSAGE, GCN, GIN, and GAT. Our impossibility results also extend to

more powerful variants that provide to each node information about the layout of its neighbors, e.g. via a *port numbering*, like CPNGNN (Sato et al., 2019), or geometric information, like DimeNet (Klicpera et al., 2020).

(2) We introduce a novel graph-theoretic formalism for analyzing CPNGNNs, and our constructions provide insights that may facilitate the design of more effective GNNs.

(3) We provide the first data dependent generalization bounds for message passing GNNs. Our guarantees are significantly tighter than the VC bounds established by Scarselli et al. (2018) for a class of GNNs. Interestingly, the dependence of our bounds on parameters is comparable to Rademacher bounds for recurrent neural networks (RNNs). Our results also hold for *folding networks* (Hammer, 2001) that operate on tree-structured inputs.

(4) Our generalization analysis specifically accounts for local permutation invariance of the GNN aggregation function. This relies on a specific sum form that extends to aggregating *port-numbered* messages, and therefore opens avenues for analyzing generalization of CPNGNNs.

The rest of the paper is organized as follows. Related work is presented in section 2. We provide the necessary background material in section 3. We elucidate the limitations of different GNN variants, introduce our graph-theoretic formalism, and propose a more powerful variant than CPNGNN and DimeNet in section 4. Finally, we establish generalization bounds for GNNs in section 5. We outline some key steps of our results in the main text, and defer the details of the proofs to the Supplementary material.

2 Related Work

GNNs continue to generate much interest from both theoretical and practical perspectives. An important theoretical focus has been on understanding the expressivity of existing architectures, and thereby introducing richer (invariant) models that can generate more nuanced embeddings. But, much less is known about the generalization ability of GNNs. We briefly review some of these works.

Expressivity. Scarselli et al. (2009) extended the universal approximation property of feed-forward networks (FFNs) (Scarselli and Tsoi, 1998) to GNNs using the notion of *unfolding equivalence*. Recurrent neural operations for graphs have been introduced with their associated kernel spaces (Lei et al., 2017). Dai et al. (2016) performed a sequence of mappings inspired by mean field and belief propagation procedures from graphical models, and Gilmer et al. (2017) showed that common graph neural net models may be studied as Message Passing Neural Networks (MPNNs). It is known (Xu et al., 2019) that GNN variants such as GCNs (Kipf and Welling, 2017) and GraphSAGE (Hamilton et al., 2017) are no more discriminative than the Weisfeiler-Lehman (WL) test. In order to match the power of the WL test, Xu et al. (2019) also proposed GINs. Showing GNNs are not powerful enough to represent probabilistic logic inference, Zhang et al. (2020) introduced *ExpressGNN*. Among other works, Barceló et al. (2020) proved results in the context of first order logic, and Dehmamy et al. (2019) investigated GCNs through the lens of graph moments underscoring the importance of depth compared to width in learning higher order moments. The inability of some graph kernels to distinguish graph properties such as planarity has also been established (Kriege et al., 2018, 2020).

Spatial, hierarchical, and higher order GNN variants have also been explored. Notably, Sato et al. (2019) exploited a local port ordering of nodes to introduce Consistent Port Numbering GNN (CPNGNN), which they proved to be strictly more powerful than WL. They and Loukas (2020) also established connections to distributed local algorithms. Higher order generalizations have been studied by (Morris et al., 2019; Murphy et al., 2019; Maron et al., 2019c); in particular, Maron et al. (2019a) introduced models that are more powerful than WL. Hella et al. (2015) investigated models weaker than port numbering. Several other works exploit spatial information to obtain more nuanced embeddings (Ying et al., 2018; You et al., 2019; Ingraham et al., 2019; Klicpera et al., 2020; Chen et al., 2019b). Xu et al. (2018) learned locally adaptive structure-aware representations by adaptively aggregating information over extended neighborhoods. Veličković et al. (2018) introduced GATs that obviate specifying the graph structure in advance.

Invariance. An important consideration in the design of GNNs is their ability to produce output embeddings that are equivariant or permutation-invariant to the input feature vectors. Maron et al. (2019b) constructed permutation-invariant and equivariant linear layers, and showed that their model can approximate any GNN that can be cast as a MPNN in the framework of Gilmer et al. (2017). Murphy et al. (2019) constructed new permutation-invariant functions for variable-size inputs, and suggested some approximations. Maron et al. (2019c); Keriven and Peyré (2019) proved universality theorems for a specific class of invariant and equivariant networks, respectively.

Generalization. Several works have established generalization guarantees for FFNs (Bartlett et al., 2017; Golowich et al., 2018; Neyshabur et al., 2018; Zhang et al., 2018a) and RNNs (Chen et al., 2019a; Allen-Zhu and Li, 2019). GNNs differ in some key aspects from those models. Unlike RNNs that process sequences, GNNs operate on graph-structured data: sharing of recurrent weights takes place along both the depth and width of a GNN. Unlike FFNs, GNNs deal with irregular local structure. Moreover, at each node, GNNs typically employ permutation-invariant aggregations, in contrast to global permutation invariance (Sokolic et al., 2017). Scarselli et al. (2018) proved VC-dimension bounds for GNNs on a restricted class of graphs that have their label determined by a single designated node. Verma and Zhang (2019) showed stability bounds for single-layer GCNs in a semi-supervised setting.

3 Preliminaries

We define the shorthand $[c] = \{1, 2, \dots, c\}$. For a matrix W , we denote its Frobenius norm by $\|W\|_F$ and spectral norm by $\|W\|_2$. We also denote the Euclidean norm of a vector v by $\|v\|_2$.

In a popular class of GNNs, which we call *Locally Unordered* GNNs (LU-GNNs), the embedding of each node is updated using messages from its neighbors but without using any spatial information (e.g., the relative orientation of the neighbors). This class subsumes variants such as GraphSAGE (Hamilton et al., 2017), GCN (Kipf and Welling, 2017), GIN (Xu et al., 2019), and GAT (Veličković et al., 2018). We can summarize the updated embedding $h_v^{(\ell)}$ for node v at layer ℓ in many LU-GNNs by an aggregation and combine operation:

$$\begin{aligned}\tilde{h}_v^{(\ell-1)} &= \text{AGG}\{h_u^{(\ell-1)} | u \in N(v)\}, \\ h_v^{(\ell)} &= \text{COMBINE}\{h_v^{(\ell-1)}, \tilde{h}_v^{(\ell-1)}\},\end{aligned}$$

where $N(v)$ denotes the set of neighbors of v , and functions AGG and COMBINE are sometimes folded into a single aggregation update. These models are often implemented as MPNNs (Dai et al., 2016; Gilmer et al., 2017). One common implementation, called *mean field embedding* (Dai et al., 2016), uses the input features x_v of node v , in place of $h_v^{(\ell-1)}$ in the COMBINE step above; we will use an instance of this variant for generalization analysis. AGG is typically a permutation-invariant function (e.g., sum).

Recently, two subtle variants have been proposed that exploit local structure to treat the neighbors differently. One of these, CPNGNN (Sato et al., 2019), is based on a *consistent port numbering* that numbers the neighbors of each node v from $1 \dots \text{degree}(v)$. Equivalently, a *port numbering* (or *port ordering*) function p associates with each edge (u, v) a pair of numbers (i, j) , $i \in [\text{degree}(u)]$ and $j \in [\text{degree}(v)]$ such that $p(u, i) = (v, j)$, i.e., u is *connected* to v via *port* i . Thus, u can tell any neighbor from the others based on its ports. We say p is *consistent* if $p(p(u, i)) = (u, i)$ for all (u, i) . Multiple consistent orderings are feasible; CPNGNN arbitrarily fixes one before processing the input graph.

When computing node embeddings, the embedding of node v is updated by processing the information from its neighbors as an *ordered* set, ordered by the port numbering, i.e., the aggregation function is generally not permutation invariant. In addition to a neighbor node u 's current embedding, v receives the port number that connects u to v .

Another model, *DimeNet* (Klicpera et al., 2020), is a *directional* message passing algorithm introduced in the context of molecular graphs. Specifically, DimeNet embeds atoms via a set of messages (i.e., edge

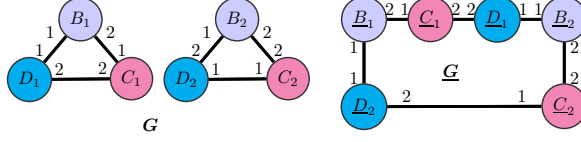


Figure 1: **Construction for Proposition 1.** Graph \mathbf{G} consists of two triangles that differ in ports (shown next to nodes on each edge) but are otherwise identical, whereas $\underline{\mathbf{G}}$ consists of a 6-cycle. LU-GNNs do not use ports, and each node treats all its messages equally. Thus, the neighborhood of each node X_1 , where $X \in \{B, C, D\}$ in \mathbf{G} , is indistinguishable from that of \underline{X}_1 in $\underline{\mathbf{G}}$ (so X_1 and \underline{X}_1 have identical embeddings), and similarly X_2 and \underline{X}_2 cannot be told apart. So, LU-GNN with permutation-invariant readout fails to separate \mathbf{G} and $\underline{\mathbf{G}}$. In contrast, CPNGNN can exploit that port 2 of D_2 connects it to B_2 , whereas the corresponding node \underline{D}_2 connects to \underline{B}_1 via port 1.

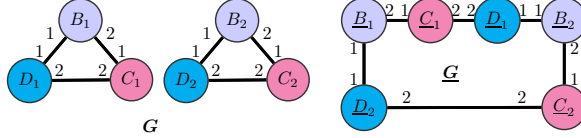


Figure 2: **Construction for Proposition 2.** Graphs \mathbf{G} and $\underline{\mathbf{G}}$ are same as in Fig. 1, but have been assigned a different consistent numbering. CPNGNN can no longer distinguish the graphs with permutation-invariant readout since each node labeled with X_1 in \mathbf{G} , where $X \in \{B, C, D\}$ has a corresponding node labeled \underline{X}_1 in $\underline{\mathbf{G}}$ with identical features and indistinguishable port-numbered neighborhoods (similarly for X_2). Thus, ordering matters.

embeddings) and leverages the directional information by transforming messages based on the angle between them. For each node v , the embedding for an incoming message from neighbor u is computed as

$$m_{uv}^{(\ell)} = f_1(m_{uv}^{(\ell-1)}, \tilde{m}_{uv}^{(\ell-1)}), \quad \text{where} \quad (1)$$

$$\tilde{m}_{uv}^{(\ell-1)} = \sum_{w \in N(u) \setminus \{v\}} f_2(m_{wu}^{(\ell-1)}, e^{(uv)}, a^{(wu, uv)}) ,$$

and $e^{(uv)}$ is a representation of the distance from u to v , $a^{(wu, uv)}$ combines $\angle wuv$ with the distance from w to u , and f_1 and f_2 are update functions similar to AGG and COMBINE. The node embedding $h_v^{(\ell)}$ is simply the sum of message embeddings $m_{uv}^{(\ell)}$.

For a specified graph property P and readout function f , we say that a GNN Q *decides* P , if for any pair of graphs (G_1, G_2) such that G_1 and G_2 differ on P , we have $f(g_Q(G_1)) \neq f(g_Q(G_2))$. Here, $g_Q(G)$ denotes the collection of embeddings of nodes in G when G is provided as input to Q . We consider several important graph properties in this paper: (a) *girth* (length of the shortest cycle), (b) *circumference* (length of the longest cycle), (c) *diameter* (maximum distance, in terms of shortest path, between any pair of nodes in the graph), (d) *radius* (minimum node eccentricity, where eccentricity of a node u is defined as the maximum distance from u to other vertices), (e) *conjoint cycle* (two cycles that share an edge), (f) *total number of cycles*, and (g) *k-clique* (a subgraph of at least $k \geq 3$ vertices such that each vertex in the subgraph is connected by an edge to any other vertex in the subgraph).

4 Representation limits of GNNs

We now sketch novel constructions to illustrate the limits of LU-GNNs, CPNGNNs, and DimeNets. First, we show that in some cases, CPNGNNs can be more discriminative than LU-GNNs, depending on the port numbering. Then, we demonstrate that still, LU-GNNs, CPNGNNs, and DimeNets cannot compute certain graph properties. Our proofs build examples of graphs that (1) differ in important graph properties, but that (2) these models cannot distinguish. As a consequence, these models will not be able to compute such

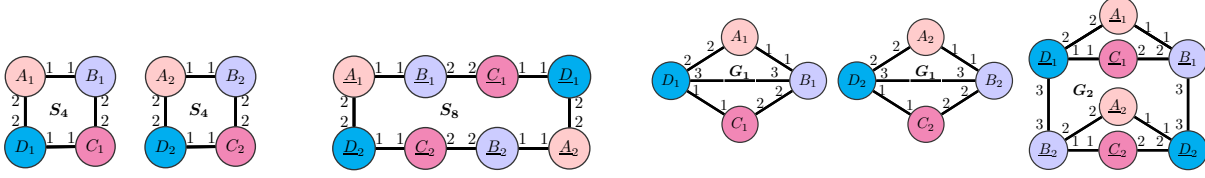


Figure 3: **Constructions for Proposition 4.** The graph with two copies of \underline{S}_4 is indistinguishable from S_8 despite having different girth, circumference, diameter, radius, and total number of cycles. This follows since for each $X \in \{A, B, C, D\}$, nodes X_1 and \underline{X}_1 have identical feature vectors as well as identical port-ordered neighborhoods (similarly for nodes X_2 and \underline{X}_2). Likewise, the graph with two copies of \underline{G}_1 , each having a conjoint cycle, cannot be distinguished from G_2 as the graphs are port-locally isomorphic. A simple modification extends the result to k -clique (described in the Supplementary). The constructions hold for LU-GNNs as well (by simply ignoring the port numbers). Note that, in contrast, DimeNet is able to distinguish the graphs in these constructions, e.g., using that $\angle A_1 B_1 C_1$ is different from the corresponding $\angle \underline{A}_1 \underline{B}_1 \underline{C}_1$.

graph properties in general.

To formalize this framework, we introduce a condition of local isomorphism for a pair of graphs. This condition implies that CPNGNNs and LU-GNNs cannot distinguish the two graphs. A similar framework applies to DimeNet. Finally, our insights point to a new GNN variant that leverages additional geometric features to circumvent our constructions for CPNGNNs and DimeNets.

Limitations of LU-GNNs.

Proposition 1. *There exist some graphs that LU-GNNs cannot distinguish, but CPNGNN can distinguish with some consistent port ordering.*

Fig. 1 shows two graphs, G (consisting of two triangles) and \underline{G} . Nodes with same color (or, equivalently, same uppercase symbol without the subscripts and underline) have identical feature vectors. The port numbers for each node are shown next to the node on the respective edges (note the numbering is consistent). Moreover, for LU-GNNs, edges on nodes with same color have identical edge feature vectors; for CPNGNNs, edge features are the same if, in addition, the local ports for nodes that have the same color are identical. As explained in Fig. 1, CPNGNN can distinguish between the two graphs by exploiting the port information. However, LU-GNNs do not leverage such information, and fail to find distinct representations.

Limitations of CPNGNNs. Port orderings help CPNGNNs distinguish graphs better. But, port orderings are not unique, and not all orderings distinguish the same set of graphs.

Proposition 2. *There exist pairs of graphs and consistent port numberings p and q such that CPNGNN can distinguish the graphs with p but not q .*

Fig. 2 shows the same pair of graphs G and \underline{G} but with a different ordering. CPNGNN can no longer distinguish the two non-isomorphic graphs with this new ordering. Therefore, it may be useful to try multiple random orderings, or even parameterize and learn one along with other GNN parameters.

Henceforth, we assume that an ordering is given with the input graph. We now demonstrate the inability of CPNGNNs to decide several graph properties. Toward that goal, note that in Fig. 1 we conjured an explicit bijection between nodes in G and \underline{G} to reason about permutation-invariant readouts. We now introduce a graph-theoretic formalism for CPNGNNs that obviates the need for an explicit bijection and is easier to check.

We define a pair of surjective mappings between two graphs in question, and impose additional conditions that guarantee the existence of a bijection. This bijection implies that corresponding nodes in the graphs

receive identical embeddings, and hence both graphs obtain the same set of node embeddings, making them indistinguishable.

The main idea is that a node v_1 in graph G_1 is locally indistinguishable from v_2 in G_2 if (1) the node features agree: $x_{v_1} = x_{v_2}$, and (2) the port-ordered local neighborhoods of v_1 and v_2 cannot be told apart. That is, if port i of v_1 connects to port k of v , then a locality preserving bijection connects the nodes corresponding to images of v_1 and v via the same ports. In the notation here, we include the port numbers (i, j) associated with each edge (u, v) in the edge notation, i.e., $((u, i), (v, j))$.

Definition 1. We say that graph $G_1(V_1, E_1, p)$ *port-covers* $G_2(V_2, E_2, q)$ if the following conditions are satisfied: **(a)** there exists a surjection $f : V_1 \mapsto V_2$ such that $x_v = x_{f(v)}$ for all $v \in V_1$, **(b)** p and q are consistent, and **(c)** for all $v_1 \in V_1$ there exists a local bijection g_{v_1} such that for all $i \in [\text{degree}(v_1)]$ and $(v, k) = p(v_i, i)$, we have

$$g_{v_1}(((v_1, i), (v, k))) = (q(f(v), k), q(f(v_1), i)) ,$$

such that $q(f(v), k) = (f(v_1), i)$; $q(f(v_1), i) = (f(v), k)$; $((v_1, i), (v, k)) \in E_1$; and $(q(f(v), k), q(f(v_1), i)) \in E_2$. Moreover, we say that $G_1(V_1, E_1, p)$ and $G_2(V_2, E_2, q)$ are *port-locally isomorphic* if they both cover each other.

Note that Definition 1 does not preclude the possibility that f maps multiple nodes in G_1 to the same node in G_2 , or the other way round. That being the case, the claim that G_1 and G_2 cannot be distinguished by CPNGNN might not hold. Fortunately, the following result comes to our rescue.

Proposition 3. *If $G_1(V_1, E_1, p)$ and $G_2(V_2, E_2, q)$ are port-locally isomorphic, there exists a bijection h that satisfies **(a)**-**(c)** in Definition 1 (with h replacing f). As a corollary, CPNGNNs produce identical embeddings for the corresponding nodes in G_1 and G_2 , so CPNGNNs cannot separate G_1 and G_2 with permutation-invariant readout.*

We now proceed to establish that CPNGNNs are limited in that they fail to decide important graph properties. We can invoke conditions of Proposition 3, or define a bijection, to show the following result (see Fig. 3 for our constructions).

Proposition 4. *There exist consistent port orderings such that CPNGNNs with permutation-invariant readout cannot decide several important graph properties such as girth, circumference, diameter, radius, conjoint cycle, total number of cycles, and k -clique.*

Clearly, these impossibility results apply to LU-GNNs as well (see Fig. 3). However, as described in Fig. 3, our constructions for CPNGNNs do not work for DimeNets. This immediately leads us to the question whether DimeNets are expressive enough to decide the graph properties.

Limitations of DimeNets. Unfortunately, as we show in Fig. 4, it turns out we can craft another construction on two graphs that differ in several of these properties but cannot be distinguished by DimeNets.

Proposition 5. *DimeNet with permutation-invariant readout cannot decide graph properties such as girth, circumference, diameter, radius, or total number of cycles.*

In fact, as we argue in Fig. 4, augmenting DimeNet with port-numbering would still not be sufficient. Therefore, a natural question that arises is whether we can obtain a more expressive model than both CPNGNN and DimeNet. Leveraging insights from our constructions, we now introduce one such variant, *H-DCPN* (short for *Hierarchical Directional Message Passing Consistent Port Numbering Networks*), that generalizes both CPNGNN and DimeNet.

More powerful GNNs. The main idea is to augment DimeNet not just with port ordering, but also additional spatial information. Observe that the construction in Fig. 4 will fail if for each edge (u, v) , we additionally model the set of angles α_{wuvz} between planes $\mathcal{P}(w, u, v)$ and $\mathcal{P}(u, v, z)$ due to neighbors w of u and neighbors z of v . Similarly, we could use the distances between these planes. We denote by Φ_{uv} all such features due to these planes. Denote by $m_{uv}^{(\ell)}$ the message from neighbor u of v at time ℓ , and by

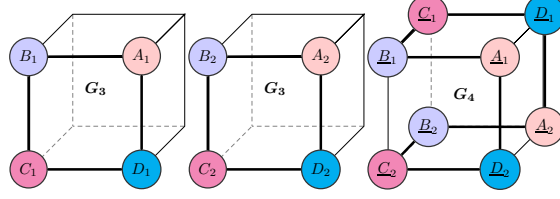


Figure 4: **Construction for Proposition 5.** DimeNet cannot discriminate between \mathbf{G}_4 and the other graph that consists of two identical copies of \mathbf{G}_3 , since the corresponding local angles and distances are identical in the two graphs. Moreover, since \mathbf{G}_3 and \mathbf{G}_4 are obtained by overlaying \mathbf{S}_4 and \mathbf{S}_8 (from Fig. 3), respectively on a cube, augmenting DimeNet with the port-numbering scheme from \mathbf{S}_4 and \mathbf{S}_8 will still not be sufficient to distinguish the graphs.

$\underline{m}_{uv}^{(\ell)} = \underline{f}(m_{uv}^{(\ell)}, \Phi_{uv})$ a refined message that encapsulates the effect of geometric features.

We incorporate salient aspects of CPNGNN as well. Specifically, we first fix a consistent port numbering, as in CPNGNN. Denote the degree of v by $d(v)$. Let $c_v(j)$ be the neighbor of v that connects to port j of v via port $t_{j,v}$, for $j \in [d(v)]$. We suggest to update the embedding of v as

$$h_v^{(\ell)} = f(h_v^{(\ell-1)}, \underline{m}_{c_v(1)v}^{(\ell-1)}, t_{1,v}, \dots, \underline{m}_{c_v(d(v))v}^{(\ell-1)}, t_{d(v),v}),$$

where f can potentially take into account the ordering of its arguments. The update resembles CPNGNN when we define $m_{uv}^{(\ell)} = h_u^{(\ell)}$; and DimeNet when f ignores $h_v^{(\ell-1)}$ (and ports) and we define $m_{uv}^{(\ell)}$ using (1) in section 3. H-DCPN derives its additional discriminative power from the features Φ_{uv} encoded in messages $\underline{m}_{uv}^{(\ell)}$. For instance, the nodes labeled A_1, B_1, C_1, D_1 lie on the same plane in \mathbf{G}_3 . In contrast, the plane defined by nodes with labels $\underline{A}_1, \underline{B}_1, \underline{C}_1$ in \mathbf{G}_4 is orthogonal to that defined by nodes with labels $\underline{D}_2, \underline{A}_1, \underline{B}_1$; thus allowing H-DCPN to distinguish the node labeled A_1 from the node labeled \underline{A}_1 (Fig. 4).

5 Generalization bounds for GNNs

Next, we study the generalization ability of GNNs via Rademacher bounds, focusing on binary classification. We generalize the previous results on the complexity of feedforward networks (Bartlett et al., 2017; Neyshabur et al., 2018) and RNNs (Chen et al., 2019a) in mainly three ways. First, we process graphs unlike sequences in RNNs, or instances restricted to the input layer in feedforward networks. Toward that goal, we show the complexity of GNNs that combine predictions from individual nodes may be analyzed by focusing on local node-wise computation trees. Second, we share weights across all nodes in these computation trees (i.e., both along the depth and the width of the tree). Third, we model *local* permutation-invariance in the aggregate function at each node in the tree. Our bounds are comparable to the Rademacher bounds for RNNs.

We consider locally permutation invariant GNNs, where in each layer ℓ , the embedding $h_v^\ell \in \mathbb{R}^r$ of node v of a given input graph is updated by aggregating the embeddings of its neighbors, $u \in N(v)$, via an aggregation function $\rho: \mathbb{R}^r \rightarrow \mathbb{R}^r$. Different types of updates are possible; we focus on a *mean field* update (Dai et al., 2016; Jin et al., 2018, 2019):

$$h_v^\ell = \phi(W_1 x_v + W_2 \rho(\sum_{u \in N(v)} g(h_u^{\ell-1}))), \quad (2)$$

where ϕ and g are nonlinear transformations and $x_v \in \mathbb{R}^r$ is the feature vector for v . We assume $\rho(0) = 0$, $\|x_v\|_2 \leq B_x$ for all v , $\|\phi(x)\|_\infty \leq b < \infty$ for all $x \in \mathbb{R}^r$, $\phi(0) = 0$, $g(0) = 0$. One possible choice of ϕ is a squashing function such as tanh. We also assume that ϕ , ρ , and g have Lipschitz constants C_ϕ , C_ρ , and C_g respectively; and that W_1 and W_2 have bounded norms: $\|W_1\|_2 \leq B_1$, $\|W_2\|_2 \leq B_2$. The weights W_1, W_2 and functions ϕ, ρ, g are shared across nodes and layers.

The graph label is generated by a readout function that aggregates node embeddings of the final layer L . Here, we assume this function applies a local binary classifier of the form $f_c(h_v^L) = \psi(\beta^\top h_v^L)$ from a family \mathcal{F}_β parameterized by β such that $\|\beta\|_2 \leq B_\beta$, with sigmoid function ψ to each node representation h_v^L , and then averages the binary predictions of all nodes, i.e., $f(G) = \sum_{v \in V} f_c(h_v^L)$. We predict label 1 if $f(G) > 0.5$, else 0. Such networks implement permutation invariance locally in each neighborhood, and globally when aggregating the node embeddings. This invariance will play an important role in the analysis.

Let $f(G)$ be the output of the entire GNN for input graph G with true label $y \in \{0, 1\}$. Our loss is a margin loss applied to the difference in probability between true and incorrect label:

$$p(f(G), y) = y(2f(G) - 1) + (1 - y)(1 - 2f(G)),$$

with $p(f(G), y) < 0$ if and only if there is a classification error. The margin loss is then, with $a = -p(f(G), y)$ and indicator function $\mathbf{1}[\cdot]$:

$$\text{loss}_\gamma(a) = \mathbf{1}[a > 0] + (1 + a/\gamma)\mathbf{1}[a \in [-\gamma, 0]]. \quad (3)$$

A standard result in learning theory relates the population risk $\mathbb{P}[p(f(G), y) \leq 0]$ to the empirical risk for training examples $\{(G_j, y_j)\}_{j=1}^m$

$$\hat{\mathcal{R}}_\gamma(f) = \frac{1}{m} \sum_{j=1}^m \text{loss}_\gamma(-p(f(G_j), y_j)) \quad (4)$$

and the empirical Rademacher complexity $\hat{\mathcal{R}}_S(\mathcal{J}_\gamma)$ of the class \mathcal{J}_γ of functions concatenating the loss with the GNN prediction function f .

Lemma 1 (Mohri et al. (2012)). *For any margin $\gamma > 0$, any prediction function f in a class \mathcal{F} and $\mathcal{J}_\gamma \in \{(G, y) \mapsto \text{loss}_\gamma(-p(f(G), y)) | f \in \mathcal{F}\}$, given m samples $(G_j, y_j) \sim \mathcal{D}$, with probability $1 - \delta$, the population risk for \mathcal{D} and f is bounded as*

$$\mathbb{P}(p(f(G), y) \leq 0) \leq \hat{\mathcal{R}}_\gamma(f) + 2\hat{\mathcal{R}}_G(\mathcal{J}_\gamma) + 3\sqrt{\frac{\log(2/\delta)}{2m}}.$$

Hence, we need to bound the empirical Rademacher complexity $\hat{\mathcal{R}}_G(\mathcal{J}_\gamma)$ for GNNs. We do this in two steps: (1) we show that it is sufficient to bound the Rademacher complexity of local node-wise computation trees; (2) we bound the complexity for a single tree via recursive spectral bounds, taking into account permutation invariance.

5.1 From Graphs to Trees

We begin by relating the Rademacher complexity of \mathcal{J}_γ to the complexity of each node classification. The node embedding h_v^L is equal to a function applied to the local computation tree of depth L , rooted at v , that we obtain when unrolling the L neighborhood aggregations. That is, the tree represents the structured L -hop neighborhood of v , where the children of any node u in the tree are the nodes in $N(u)$. Hence, if t is the tree at v , we may write, with a slight abuse of notation, $f_c(h_v^L) = f_c(t; \Theta)$, where Θ represents the parameters W_1, W_2 of the embedding and β of the node classifier.

With this notation, we rewrite $f(G; \Theta)$ as an expectation over functions applied to trees. Let T_1, \dots, T_n be the set of all possible computation trees of depth L , and $w_i(G)$ the number of times T_i occurs in G . Then, note that we may write $f(G; \Theta)$ as the sum

$$\sum_{i=1}^n \frac{w_i(G)}{\underbrace{\sum_{\ell=1}^n w_\ell(G)}_{= w'_i(G)}} f_c(T_i; \Theta) = \mathbb{E}_{T \sim w'(G)} f_c(T; \Theta). \quad (5)$$

This perspective implies a key insight of our analysis: the complexity of the GNN may be bounded by the complexity of the computation trees.

Proposition 6. Let $\mathcal{G} = \{G_1, \dots, G_m\}$ be a set of i.i.d. graphs, and let $\mathcal{T} = \{t_1, \dots, t_m\}$ be such that $t_j \sim w'(G_j), j \in [m]$. Denote by $\hat{\mathcal{R}}_{\mathcal{G}}$ and $\hat{\mathcal{R}}_{\mathcal{T}}$ the empirical Rademacher complexity of GNNs for graphs \mathcal{G} and trees \mathcal{T} , respectively. Then $\hat{\mathcal{R}}_{\mathcal{G}} \leq \mathbb{E}_{t_1, \dots, t_m} \hat{\mathcal{R}}_{\mathcal{T}}$.

Therefore, to apply Lemma 1, it is sufficient to bound the Rademacher complexity of classifying single node-wise computation trees. Before addressing this next step in detail, we state and discuss our main result for this section.

5.2 Generalization Bound for GNNs

We define the *percolation complexity* of our GNNs to be $\mathcal{C} \triangleq C_\rho C_g C_\phi B_2$. We now bound $\hat{\mathcal{R}}_{\mathcal{T}}(\mathcal{J}_\gamma)$, when each tree $t_j \in \mathcal{T}$ has a branching factor (i.e., maximum number of neighbors for any node) at most d , and \mathcal{J}_γ maps each (t, y) pair to $\text{loss}_\gamma(-p(f_c(t; \Theta), y))$.

Proposition 7. The empirical Rademacher complexity of \mathcal{J}_γ with respect to \mathcal{T} is

$$\begin{aligned} \hat{\mathcal{R}}_{\mathcal{T}}(\mathcal{J}_\gamma) &\leq \frac{4}{\gamma m} + \frac{24rB_\beta Z}{\gamma\sqrt{m}} \sqrt{3 \log Q}, \quad \text{where} \\ Q &= 24B_\beta \sqrt{m} \max\{Z, M\sqrt{r} \max\{B_x B_1, \overline{R} B_2\}\}, \\ M &= C_\phi \frac{(Cd)^L - 1}{Cd - 1}, \quad Z = C_\phi B_1 B_x + C_\phi B_2 \overline{R}, \\ \overline{R} &\leq C_\rho C_g d \min\{b\sqrt{r}, B_1 B_x M\}. \end{aligned}$$

Note that we do not need to prespecify B_1 and B_2 : we can simply take these values to be the spectral norm, respectively, of the learned weights W_1 and W_2 . Before proceeding with the proof, we discuss some important implications of this result in the wake of Lemma 1 and Proposition 6.

Comparison with RNN. We summarize below the dependence of our generalization error on the various parameters for different \mathcal{C} up to log factors (denoted by notation $\tilde{\mathcal{O}}$). We also mention the corresponding bounds for RNN on a sequence of length L when the spectral norm of recurrent weights in RNN is respectively less than, equal to, or greater than 1 (note that we renamed some parameters from Chen et al. (2019a) for notational consistency). Our analysis implies GNNs have essentially the same dependence on dimension r ,

\mathcal{C}	GNN (ours)	RNN (Chen et al. (2019a))
$< 1/d$	$\tilde{\mathcal{O}}\left(\frac{rd}{\sqrt{m}\gamma}\right)$	$\tilde{\mathcal{O}}\left(\frac{r}{\sqrt{m}\gamma}\right)$
$= 1/d$	$\tilde{\mathcal{O}}\left(\frac{rdL}{\sqrt{m}\gamma}\right)$	$\tilde{\mathcal{O}}\left(\frac{rL}{\sqrt{m}\gamma}\right)$
$> 1/d$	$\tilde{\mathcal{O}}\left(\frac{rd\sqrt{rL}}{\sqrt{m}\gamma}\right)$	$\tilde{\mathcal{O}}\left(\frac{r\sqrt{rL}}{\sqrt{m}\gamma}\right)$

depth L , and sample size m as RNN. The additional dependence on branching factor d is due to processing trees, in contrast to processing sequences in RNNs.

Comparison with VC-bounds for GNNs. Scarselli et al. (2018) proved that the dependence of VC-dimension in their setting for tanh and logistic sigmoid activations is fourth order with respect to the number of hidden units H , and quadratic in each of r and maximum number of nodes N in any input graph. Note that N is at least d , and possibly much larger than d . Since $H = r$ in our setting, this amounts to having VC-dimension scale as $\mathcal{O}(r^6 N^2)$, and consequently, generalization error scale as $\tilde{\mathcal{O}}(r^3 N / \sqrt{m})$. Thus, our generalization bounds are significantly tighter even when $L = \mathcal{O}(r)$.

Role of local permutation invariance. Note that previous works were confined to dealing with permutation-invariance at a global level (Sannai and Imaizumi (2019); Sokolic et al. (2017)). In contrast, we perform a composition of permutation-invariant transformations, where each transformation pertains to applying a permutation at a level of the input tree. We exploit local permutation-invariance via sum-decomposability. In the absence of local permutation-invariance, we would need to deal with the orderings at each node separately.

Extension to other variants. Note that we define C_g and C_ρ with respect to the aggregate function (e.g., unweighted sum or mean) that acts prior to transformation by W_2 . We can easily extend our analysis to include the edge embeddings. We considered message passing in the context of so-called *mean field embedding* (Dai et al., 2016), however, other updates, such as *embedded loopy belief propagation*, may be analyzed similarly in our framework.

Analysis. Our proof follows a multistep analysis. We first quantify the effect of change in shared variables on the embedding of the root node of a fixed tree. This step entails a recursive decomposition over the effect on subtrees. Specifically, we recursively bound the effect on each subtree of the root by the maximum effect across these subtrees. Since both the non-linear activation function and the permutation-invariant aggregation function are Lipschitz-continuous, and the feature vector at the root and the shared weights have bounded norm, the embedding at the root of the tree adapts to the embeddings from the subtrees. We then quantify the effect of changing not only the shared weights but also changing the classifier parameters. Since the classifier parameters are chosen from a bounded norm family, we can bound the change in prediction probability. This allows us to use a covering number argument to approximate the predictions, and subsequently, bound the empirical Rademacher complexity via Dudley’s entropy integral.

Fix the feature vectors for the computation tree of depth L having degree of each internal node equal to d . Let the feature vector associated with the root (assumed to be at level L) of the tree be given by x_L . We denote the feature vector associated with node j at level $\ell \in [L - 1] \triangleq \{1, 2, \dots, L - 1\}$ by $x_{\ell,j}$. Denote the embedding produced by the subtree rooted at node j on level $\ell \in [L - 1]$ by $T_{\ell,j}(W_a, W_b)$ when W_a and W_b are the parameters of the model. Consider two sets of parameters $\{W_1, W_2\}$ and $\{W'_1, W'_2\}$. We will denote the embedding vector produced by the GNN after processing the entire tree by $T_L(W_1, W_2)$ as a shorthand for $T_{L,1}(W_1, W_2)$. Denote the set of subtrees of node with feature vector x by $C(x)$. We structure the proof as a sequence of several sub-results for improved readability. We first quantify the change in embedding due to change in the shared weight parameters.

Lemma 2. *The l_2 -norm of difference of embedding vectors produced by (W_1, W_2) and (W'_1, W'_2) after they process the tree all the way from the leaf level to the root can be bounded recursively as*

$$\begin{aligned} \Delta_L &\triangleq \|T_L(W_1, W_2) - T_L(W'_1, W'_2)\|_2 \\ &\leq C_\phi B_x \|(W_1 - W'_1)\|_2 + C_d \max_{j \in C(x_L)} \Delta_{L-1,j} \\ &\quad + C_\phi \|(W_2 - W'_2)R(W_1, W_2, x_L)\|_2, \end{aligned}$$

where

$$R(W_1, W_2, x_L) = \rho\left(\sum_{j \in C(x_L)} g(T_{L-1,j}(W_1, W_2))\right)$$

is the permutation-invariant aggregation of the embeddings of the subtrees rooted at level $L-1$ under (W_1, W_2) .

We therefore proceed to bounding $\|R(W_1, W_2, x_L)\|_2$.

Lemma 3.

$$\begin{aligned} &\|R(W_1, W_2, x_L)\|_2 \\ &\leq C_\rho C_g d \min \left\{ b\sqrt{r}, C_\phi B_1 B_x \frac{(Cd)^L - 1}{Cd - 1} \right\} \end{aligned}$$

We now quantify the change in probability (that the tree label is 1) Λ_L due to change in both the shared weights and the classifier parameters. We prove the following result.

Lemma 4. *The change in probability Λ_L due to change in parameters from (W_1, W_2, β) to (W'_1, W'_2, β') is*

$$\begin{aligned}\Lambda_L &= |\psi(\beta^\top T_L(W_1, W_2)) - \psi(\beta'^\top T_L(W'_1, W'_2))| \\ &\leq \|\beta - \beta'\|_2 Z + B_\beta \Delta_L,\end{aligned}$$

where Z is an upper bound on $\|T_L(W_1, W_2)\|_2$. Moreover, we can bound Δ_L non-recursively:

$$\begin{aligned}\Delta_L &\leq MB_x \|W_1 - W'_1\|_2 \\ &+ M \|R(W_1, W_2, x_L)\|_2 \|W_2 - W'_2\|_2.\end{aligned}$$

Lemma 4 allows us to ensure that Λ_L is small via a sufficiently large covering. Specifically, we show the following.

Lemma 5. *The change in probability Λ_L can be bounded by ϵ using a covering of size P , where $\log P$ is at most*

$$3r^2 \log \left(1 + \frac{6B_\beta \max\{Z, M\sqrt{r} \max\{B_x B_1, \bar{R} B_2\}\}}{\epsilon} \right).$$

Moreover, when

$$\epsilon < 6B_\beta \max\{Z, M\sqrt{r} \max\{B_x B_1, \bar{R} B_2\}\},$$

a covering of size P such that $\log P$ is at most

$$3r^2 \log \left(\frac{12B_\beta \max\{Z, M\sqrt{r} \max\{B_x B_1, \bar{R} B_2\}\}}{\epsilon} \right)$$

suffices to ensure $\Lambda_L \leq \epsilon$. Here, $\bar{R} \triangleq \|R(W_1, W_2, x_L)\|_2$, and Z, M are as defined in the statement of Proposition 7.

The remaining steps for Proposition 7 are straightforward and deferred to the Supplementary. We now outline an approach to facilitate future work on understanding the generalization ability of CPNGNNs.

5.3 Toward generalization analysis for CPNGNNs

Two parts were integral to our analysis: **(a)** bounding complexity via local computation trees, and **(b)** the sum decomposition property of permutation-invariant functions. We now provide their counterparts for CPNGNNs.

Like before, we start with a vertex v , and unroll the L neighborhood aggregations to obtain a computation tree of depth L , rooted at v . However, now we additionally label each edge in the computation tree with the respective ports of the nodes incident on the edge (enabled by consistent ordering). Thus, we may analyze a input port-numbered graph using its node-wise port-numbered trees.

Again, note that permutation-invariance applies to multisets of messages but not port-numbered messages, therefore in CPNGNNs, we cannot express the aggregation as in (2). To address this issue, we now provide an injective function for aggregating a collection of port-numbered messages. The function takes a general sum-form that interestingly decouples the dependence on each message and its corresponding port number.

Proposition 8. *Assume \mathcal{X} is countable. There exists a function $f : \mathcal{X} \times \mathcal{P} \mapsto \mathcal{R}^n$ such that $h((x_1, p_1), \dots, (x_{|P|}, p_{|P|})) = \sum_{i \in [|P|]} g(p_i) f(x_i)$ for each port-numbered sequence of (x_i, p_i) pairs, where $P \subset \mathbb{N}$, $X = \{x_1, x_2, \dots, x_{|P|}\} \subset \mathcal{X}$ is a multiset of bounded size, and p_i are all distinct numbers from $[|P|]$.*

The result in Proposition 8 holds particular significance, since it is known (Hella et al., 2015) that port-numbered messages provide a strictly richer class than sets and multisets. The generalization bound for CPNGNN will be worse than the result in Proposition 7, since each port appears as an exponent in our generalized decomposition and thus the complexity of aggregation grows rapidly in the neighborhood size. We leave a detailed analysis of the generalization ability of CPNGNNs for future work.

References

- Z. Allen-Zhu and Y. Li. Can sgd learn recurrent neural networks with provable generalization? In *Neural Information Processing Systems (NeurIPS)*, 2019.
- P. Barceló, E. V. Kostylev, M. Monet, J Pérez, J. Reutter, and J.-P. Silva. The logical expressiveness of graph neural networks. In *International Conference on Learning Representations (ICLR)*, 2020.
- P. L. Bartlett, D. J. Foster, and M. Telgarsky. Spectrally-normalized margin bounds for neural networks. In *Advances in Neural Information Processing Systems (NIPS)*, pages 6240–6249, 2017.
- P. Battaglia, R. Pascanu, M. Lai, D. J. Rezende, and K. Kavukcuoglu. Interaction networks for learning about objects, relations and physics. In *Neural Information Processing Systems (NIPS)*, pages 4502–4510, 2016.
- M. Chen, X. Li, and T. Zhao. On generalization bounds of a family of recurrent neural networks. *arXiv : 1910.12947*, 2019a.
- Z. Chen, L. Li, and J. Bruna. Supervised community detection with line graph neural networks. In *International Conference on Learning Representations (ICLR)*, 2019b.
- H. Dai, B. Dai, and L. Song. Discriminative embeddings of latent variable models for structured data. In *International Conference on Machine Learning (ICML)*, page 2702–2711, 2016.
- M. Defferrard, X. Bresson, and P. Vandergheynst. Convolutional neural networks on graphs with fast localized spectral filtering. In *Neural Information Processing Systems (NIPS)*, pages 3844–3852, 2016.
- N. Dehmamy, A.-L. Barabasi, and R. Yu. Understanding the representation power of graph neural networks in learning graph topology. In *Neural Information Processing Systems (NeurIPS)*, pages 15387–15397, 2019.
- D. K. Duvenaud, D. Maclaurin, J. Iparraguirre, R. Bombarell, T. Hirzel, A. Aspuru-Guzik, and R. P. Adams. Convolutional networks on graphs for learning molecular fingerprints. In *Neural Information Processing Systems (NIPS)*, pages 2224–2232, 2015.
- J. Gilmer, S. S. Schoenholz, P. F. Riley, O. Vinyals, and G. E. Dahl. Neural message passing for quantum chemistry. In *International Conference on Machine Learning (ICML)*, pages 1263–1272, 2017.
- N. Golowich, A. Rakhlin, and O. Shamir. Size-independent sample complexity of neural networks. In *Conference On Learning Theory (COLT)*, pages 297–299, 2018.
- M. Gori, G. Monfardini, and F. Scarselli. A new model for learning in graph domains. In *IEEE International Joint Conference on Neural Networks (IJCNN)*, pages 729–734, 2005.
- W. Hamilton, Z. Ying, and J. Leskovec. Inductive representation learning on large graphs. In *Neural Information Processing Systems (NIPS)*, pages 1024–1034, 2017.
- B. Hammer. Generalization ability of folding networks. *IEEE Transactions on Knowledge and Data Engineering (TKDE)*, 13:196–206, 2001.
- L. Hella, M. Järvisalo, A. Kuusisto, J. Laurinharju, T. Lempiäinen, K. Luosto, J. Suomela, and J. Virtema. Weak models of distributed computing, with connections to modal logic. *Distributed Computing*, 28(1): 31–53, 2015.
- J. Ingraham, V. K. Garg, R. Barzilay, and T. Jaakkola. Generative models for graph-based protein design. In *Neural Information Processing Systems (NeurIPS)*, 2019.
- W. Jin, R. Barzilay, and T. S. Jaakkola. Junction tree variational autoencoder for molecular graph generation. In *International Conference on Machine Learning (ICML)*, volume 80, pages 2328–2337, 2018.

- W. Jin, K. Yang, R. Barzilay, and T. Jaakkola. Learning multimodal graph-to-graph translation for molecule optimization. In *International Conference on Learning Representations (ICLR)*, 2019.
- N. Keriven and G. Peyré. Universal invariant and equivariant graph neural networks. In *Neural Information Processing Systems (NeurIPS)*, pages 7090–7099, 2019.
- T. N. Kipf and M. Welling. Semi-supervised classification with graph convolutional networks. In *International Conference on Learning Representations (ICLR)*, 2017.
- J. Klicpera, J. Groß, and S. Günnemann. Directional message passing for molecular graphs. In *International Conference on Learning Representations (ICLR)*, 2020.
- N. M. Kriege, C. Morris, A. Rey, and C. Sohler. A property testing framework for the theoretical expressivity of graph kernels. In *International Joint Conference on Artificial Intelligence, IJCAI-18*, pages 2348–2354, 2018.
- N. M. Kriege, F. D. Johansson, and C. Morris. A survey on graph kernels. *Applied Network Science*, 5(1):6, 2020.
- T. Lei, W. Jin, R. Barzilay, and T. Jaakkola. Deriving neural architectures from sequence and graph kernels. In *International Conference on Machine Learning (ICML)*, pages 2024–2033, 2017.
- A. Loukas. What graph neural networks cannot learn: depth vs width. *International Conference on Learning Representations (ICLR)*, 2020.
- H. Maron, H. Ben-Hamu, H. Serviansky, and Y. Lipman. Provably powerful graph networks. In *Neural Information Processing Systems (NeurIPS)*, pages 2153–2164, 2019a.
- H. Maron, H. Ben-Hamu, N. Shamir, and Y. Lipman. Invariant and equivariant graph networks. In *International Conference on Learning Representations (ICLR)*, 2019b.
- H. Maron, E. Fetaya, N. Segol, and Y. Lipman. On the universality of invariant networks. In *International Conference on Machine Learning (ICML)*, 2019c.
- M. Mohri, A. Rostamizadeh, and A. Talwalkar. *Foundations of Machine Learning*. The MIT Press, 2012. ISBN 026201825X, 9780262018258.
- C. Morris, M. Ritzert, M. Fey, W. L. Hamilton, J. E. Lenssen, G. Rattan, and M. Grohe. Weisfeiler and leman go neural: Higher-order graph neural networks. In *AAAI Conference on Artificial Intelligence (AAAI)*, pages 4602–4609, 2019.
- R. L. Murphy, B. Srinivasan, V. A. Rao, and B. Ribeiro. Janossy pooling: Learning deep permutation-invariant functions for variable-size inputs. In *International Conference on Learning Representations (ICLR)*, 2019.
- B. Neyshabur, S. Bhojanapalli, and N. Srebro. A pac-bayesian approach to spectrally-normalized margin bounds for neural networks. In *International Conference on Learning Representations (ICLR)*, 2018.
- A. Sannai and M. Imaizumi. Improved generalization bound of permutation invariant deep neural networks. *arXiv : 1910.06552*, 2019.
- A. Santoro, F. Hill, D. Barrett, A. Morcos, and T. Lillicrap. Measuring abstract reasoning in neural networks. In *International Conference on Machine Learning (ICML)*, pages 4477–4486, 2018.
- R. Sato, M. Yamada, and H. Kashima. Approximation ratios of graph neural networks for combinatorial problems. In *Neural Information Processing Systems (NeurIPS)*, 2019.
- F. Scarselli and A. C. Tsoi. Universal approximation using feedforward neural networks: A survey of some existing methods, and some new results. *Neural Networks*, 11(1):15–37, 1998.

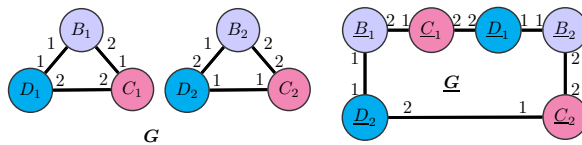
- F. Scarselli, M. Gori, A. C. Tsoi, M. Hagenbuchner, and G. Monfardini. Computational capabilities of graph neural networks. *IEEE Transactions on Neural Networks*, 20(1):81–102, 2009.
- F. Scarselli, A. C. Tsoi, and M. Hagenbuchner. The Vapnik-Chervonenkis dimension of graph and recursive neural networks. *Neural Networks*, 108:248–259, 2018.
- J. Sokolic, R. Giryes, G. Sapiro, and M. Rodrigues. Generalization Error of Invariant Classifiers. In *International Conference on Artificial Intelligence and Statistics (AISTATS)*, pages 1094–1103, 2017.
- P. Veličković, G. Cucurull, A. Casanova, A. Romero, P. Lio, and Y. Bengio. Graph attention networks. In *International Conference on Learning Representations (ICLR)*, 2018.
- S. Verma and Z.-L. Zhang. Stability and generalization of graph convolutional neural networks. In *International Conference on Knowledge Discovery & Data Mining (KDD)*, page 1539–1548, 2019.
- K. Xu, C. Li, Y. Tian, T. Sonobe, K. Kawarabayashi, and S. Jegelka. Representation learning on graphs with jumping knowledge networks. In *International Conference on Machine Learning (ICML)*, pages 5453–5462, 2018.
- K. Xu, W. Hu, J. Leskovec, and S. Jegelka. How powerful are graph neural networks? *International Conference on Learning Representations (ICLR)*, 2019.
- R. Ying, J. You, C. Morris, X. Ren, W. L. Hamilton, and J. Leskovec. Hierarchical graph representation learning with differentiable pooling. In *Neural Information Processing Systems (NeurIPS)*, 2018.
- J. You, R. Ying, and J. Leskovec. Position-aware graph neural networks. In *International Conference on Machine Learning (ICML)*, pages 7134–7143, 2019.
- S. Yun, M. Jeong, R. Kim, J. Kang, and H. Kim. Graph transformer networks. In *Neural Information Processing Systems (NeurIPS)*, pages 11960–11970, 2019.
- J. Zhang, Q. Lei, and I. S. Dhillon. Stabilizing gradients for deep neural networks via efficient SVD parameterization. In *International Conference on Machine Learning (ICML)*, pages 5801–5809, 2018a.
- M. Zhang, Z. Cui, M. Neumann, and Y. Chen. An end-to-end deep learning architecture for graph classification. In *AAAI Conference on Artificial Intelligence (AAAI)*, pages 4438–4445, 2018b.
- Y. Zhang, X. Chen, Y. Yang, A. Ramamurthy, B. Li, Y. Qi, and L. Song. Efficient probabilistic logic reasoning with graph neural networks. In *International Conference on Learning Representations (ICLR)*, 2020.

A Supplementary material

We now provide detailed proofs for all our propositions and lemmas.

Proof of Proposition 1

Proof. We show that CPNGNN, using some consistent port ordering, can distinguish some non-isomorphic graphs that LU-GNNs cannot.

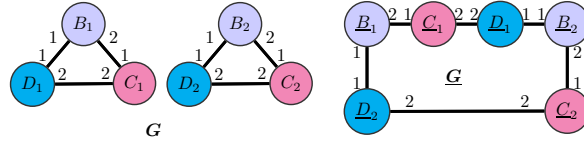


We construct a pair of graphs \mathbf{G} and $\underline{\mathbf{G}}$ such that \mathbf{G} consists of two triangles that differ in port-ordering but are otherwise identical, while $\underline{\mathbf{G}}$ (indicated by underlined symbols) consists of a single even-length cycle. The construction ensures that each node labeled with $\mathbf{X} \in \{\mathbf{B}_1, \mathbf{C}_1, \mathbf{D}_1, \mathbf{B}_2, \mathbf{C}_2\}$ in \mathbf{G} has the same identical view (i.e., indistinguishable node features, and neighborhood) as the corresponding node labeled $\underline{\mathbf{X}}$ in $\underline{\mathbf{G}}$. However, \mathbf{D}_2 and $\underline{\mathbf{D}}_2$ have distinguishable neighborhoods due to different port-numbers: e.g., \mathbf{D}_2 is connected to \mathbf{B}_2 at port 2, whereas $\underline{\mathbf{D}}_2$ is connected to $\underline{\mathbf{B}}_1$ at port 1. Likewise, \mathbf{D}_2 is connected to \mathbf{C}_2 at port 1, in contrast to $\underline{\mathbf{D}}_2$ that is connected to $\underline{\mathbf{C}}_2$ at port 2. However, LU-GNN does not incorporate any spatial information such as ports, and fails to tell one graph from the other. \square

Note that since $\angle B_1 C_1 D_1$ differs from $\angle \underline{B}_1 \underline{C}_1 \underline{D}_1$, DimeNet can also distinguish between the two graphs.

Proof of Proposition 2

Proof. We now illustrate the importance of choosing a good consistent port numbering. Specifically, we construct a pair of graphs, and two different consistent port numberings p and q such that CPNGNN can distinguish the graphs with p but not q .



We modify the consistent port numbering from the construction of Proposition 1. We consider the same pair of graphs as in the proof of Proposition 1. However, instead of having different numberings for the two components (i.e., triangles) of \mathbf{G} , we now carry over the ordering from one component to the other. The two components become identical with this modification. For any node labeled $\underline{\mathbf{X}}_1$ or $\underline{\mathbf{X}}_2$, and any neighbor labeled $\underline{\mathbf{Y}}_1$ or $\underline{\mathbf{Y}}_2$, $\mathbf{X}, \mathbf{Y} \in \{\mathbf{B}, \mathbf{C}, \mathbf{D}\}$, we can now simply assign the same respective local ports as the nodes labeled \mathbf{X}_1 and \mathbf{Y}_1 (or, equivalently, \mathbf{X}_2 and \mathbf{Y}_2). It is easy to verify that the two graphs become port-locally isomorphic under the new ordering, and thus cannot be separated with any permutation-invariant readout (using Proposition 3). \square

Proof of Proposition 3

Proof. If the surjection $f : V_1 \rightarrow V_2$ in Definition 1 is also injective, then we can simply take $h = f$. Therefore, we focus on the case when f is not injective. We will show that f can be used to inform h . Since f is not injective, there exist $v_1, v'_1 \in V_1$ such that $v_1 \neq v'_1$ but $f(v_1) = f(v'_1) = v_2$ for some $v_2 \in V_2$. Then, by condition (a) in Definition 1, we immediately get that the feature vector

$$x_{v_1} = x_{f(v_1)} = x_{f(v'_1)} = x_{v'_1} . \quad (6)$$

Moreover, by other conditions, there is a consistent port bijection from neighborhood of v_1 to that of v_2 , and likewise another bijection from neighborhood of v'_1 to that of v_2 . Therefore, there is a consistent port bijection from neighborhood of v_1 to that of v'_1 . Together with (6) and our assumption that $f(v_1) = f(v'_1) = v_2$, this implies that v_1 and v'_1 are locally *indistinguishable*. Note that there could be more such nodes that are indistinguishable from v_1 (or v'_1), e.g., when all such nodes map to v_2 as well.

Without loss of generality, let $\mathcal{E}_1(v_1) \subseteq V_1$ denote the equivalence class of all nodes, including v_1 , that are indistinguishable from v_1 in graph G_1 . Similarly, let $\mathcal{E}_2(v_2) \subseteq V_2$ be the class of nodes indistinguishable from v_2 in G_2 . Consider $\ell_1 = |\mathcal{E}_1(v_1)|$ and $\ell_2 = |\mathcal{E}_2(v_2)|$. We claim that $\ell_1 = \ell_2$. Suppose not. Then if $\ell_1 < \ell_2$, we can have h map each node in $\mathcal{E}_1(v_1)$ to a separate node in $\mathcal{E}_2(v_2)$, and use the same mapping as f on the other nodes in V_1 . Doing so does not decrease the co-domain of V_2 , and h remains surjective. We are therefore left with $\ell_2 - \ell_1 > 0$ nodes from $\mathcal{E}_2(v_2)$. Therefore, these nodes must have at least one preimage in the set $V_1 - \mathcal{E}_1(v_1)$ since f (and thus h) is a surjection by assumption (a) in Definition 1. This is clearly a contradiction since any such preimage must have either a different feature vector, or a non-isomorphic port-consistent neighborhood. By a symmetric argument, using the surjection of map from V_2 to V_1 , we conclude

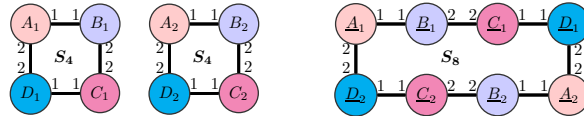
that $\ell_1 = \ell_2$. Note that h did not tinker with the nodes that were outside the class $\mathcal{E}_1(v_1)$. Recycling the procedure for other nodes in $V_1 - \mathcal{E}_1(v_1)$ that might map under f to a common image in V_2 , we note that h ends up being injective. Since h remains surjective throughout the procedure, we conclude that h is a bijection.

We now prove by induction that the corresponding nodes in port-locally isomorphic graphs have identical embeddings for any CPNGNN. Consider any such GNN with $L + 1$ layers parameterized by the sequence $\theta_{1:L+1} \triangleq (\theta_1, \dots, \theta_L, \theta_{L+1})$. Since there exists a bijection h such that any node $v_1 \in G_1$ has an identical local view (i.e., node features, and port-numbered neighbors) as $v_2 = h(v_1) \in G_2$, the updated embeddings for v_1 and v_2 are identical after the first layer. Assume that these embeddings remain identical after update from each layer $\ell \in \{2, 3, \dots, L\}$. Since v_1 and v_2 have identical local views and have identical embedding from the L th layer, the updates for these nodes by the $(L + 1)$ th layer are identical. Therefore, v_1 and v_2 have identical embeddings. Since h is a bijection, for every $v \in V_1$ there is a corresponding $h(v) \in V_2$ with the same embedding, and thus both G_1 and G_2 produce the same output with any permutation readout function. Our choice of $\theta_{1:L+1}$ was arbitrary, so the result follows. \square

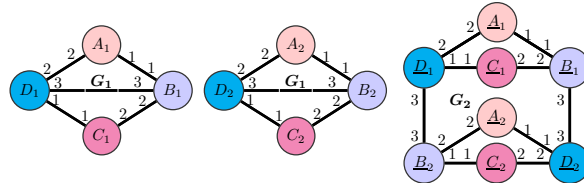
Proof of Proposition 4

Proof. We now show that there exist consistent port orderings such that CPNGNNs with permutation-invariant readout cannot decide several important graph properties: girth, circumference, diameter, radius, conjoint cycle, total number of cycles, and k -clique. The same result also holds for LU-GNNs where nodes do not have access to any consistent port numbering.

We first construct a pair of graphs that have cycles of different length but produce the same output embedding via the readout function. Specifically, we show that CPNGNNs cannot decide a graph having cycles of length n from a cycle of length $2n$. We construct a counterexample for $n = 4$. Our first graph consists of two cycles of length 4 (each denoted by S_4), while the other graph is a cycle of length 8 (denoted by S_8). We associate identical feature vectors with nodes that have the same color, or equivalently, that are marked with the same symbol ignoring the subscripts and the underline. For example, A_1 , A_2 , \underline{A}_1 , and \underline{A}_2 are all assigned the same feature vector. Moreover, we assign identical edge feature vectors to edges that have the same pair of symbols at the nodes.



Thus, we note that a bijection exists between the two graphs with node X in the first graph corresponding to \underline{X} in the second graph such that both the nodes have identical features and indistinguishable port-ordered neighborhoods. Since, the two graphs have different girth, circumference, diameter, radius, and total number of cycles, it follows from Proposition 3 that CPNGNN cannot decide these properties. Note that the graph with two S_4 cycles is disconnected, and hence its radius (and diameter) is ∞ .



We craft a separate construction for the remaining properties, namely, k -clique and conjoint cycle. The main idea is to replicate the effect of the common edge in the conjoint cycle via two identical components of another graph (that does not have any conjoint cycle) such that the components are cleverly aligned to reproduce the local port-ordered neighborhoods and thus present the same view to each node (see the adjoining figure). Specifically, each conjoint cycle is denoted by G_1 , and the other graph that does not have

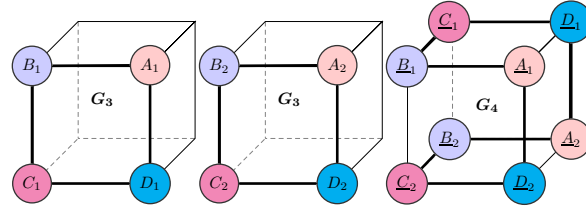
any conjoint cycles by G_2 . The graphs, being port-locally isomorphic, are indistinguishable by CPNGNN.

For the k -clique, we simply connect A_1 to C_1 , A_2 to C_2 , \underline{A}_1 to \underline{C}_1 , and \underline{A}_2 to \underline{C}_2 via a new port 3 at each of these nodes. Doing so ensures that the new graphs are port-locally isomorphic as well. Adding these edges, we note that, unlike G_2 , each conjoint cycle G_1 yields a 4-clique. \square

Proof of Proposition 5

Proof. We now demonstrate the representational limits of DimeNets. Specifically, we show two graphs that differ in several graph properties such as girth, circumference, diameter, radius, or total number of cycles. However, these graphs cannot be distinguished by DimeNets.

Note that DimeNet will be able to discriminate S_8 from the graph with cycles S_4 (recall our construction in Proposition 4), since, e.g., $\angle B_1 C_1 D_1$ in S_4 is different from $\angle \underline{B}_1 \underline{C}_1 \underline{D}_1$ in S_8 . In order to design a failure case for DimeNet, we need to construct a pair of non-isomorphic graphs that have not only identical local pairwise distances but also angles, so that their output embedding is same.



Our idea is to overlay the cycles S_4 and S_8 on a cube (see G_3 and G_4 - the graphs consist of only edges in bold). Doing so does not have any bearing on the graph properties. Since we orient the edges of these cycles along the sides of the cube, the local distances are identical. Moreover, by having $A_1 B_1 C_1 D_1$ and $A_2 B_2 C_2 D_2$ as opposite faces of the cube, we ensure that each angle in G_4 is a right angle, exactly as in G_3 . Thus, for each $X \in \{A, B, C, D\}$, nodes X_1 , X_2 , \underline{X}_1 , and \underline{X}_2 have identical feature vectors and identical local spatial information. Thus, the embeddings for X_1 , X_2 , \underline{X}_1 , and \underline{X}_2 are identical, and any permutation-invariant readout results in identical output embeddings for the two graphs. \square

Proof of Proposition 6

Proof. We now show that the complexity of the GNN may be bounded by the complexity of the computation trees. In other words, the worst case generalization bound over a set of graphs corresponds to having each graph be a single computation tree.

Formally,

$$\begin{aligned}
\hat{\mathcal{R}}_G &\triangleq \mathbb{E}_\sigma \sup_{\Theta} \sum_{j=1}^m \sigma_j f(G_j; \Theta) \\
&= \mathbb{E}_\sigma \sup_{\Theta} \sum_{j=1}^m \sigma_j \mathbb{E}_{T \sim w'(G_j)} f_c(T; \Theta) \\
&\leq \mathbb{E}_\sigma \mathbb{E}_{t_1, \dots, t_m} \sup_{\Theta} \sum_{j=1}^m \sigma_j f_c(t_j; \Theta) \\
&= \underbrace{\mathbb{E}_{t_1, \dots, t_m} \mathbb{E}_\sigma \sup_{\Theta} \sum_{j=1}^m \sigma_j f_c(t_j; \Theta)}_{\hat{\mathcal{R}}_\tau},
\end{aligned}$$

where we invoked Jensen's inequality to swap the expectation with supremum for our inequality (the operation is permissible since sup is a convex function). \square

Proof of Lemma 2

Proof. Our objective here is to bound the effect of change in weights from (W_1, W_2) to (W'_1, W'_2) on the embedding of the root node of our fixed tree (that has depth L). Since non-linear activation and permutation-invariant aggregation are both Lipschitz-continuous functions, and the feature vector at the root x_L and the weights have bounded norm, the embedding at the root of the tree adapts to the embeddings from the subtrees.

Specifically, we note that the l_2 -norm of difference of embedding vectors produced by (W_1, W_2) and (W'_1, W'_2) is

$$\begin{aligned}
\Delta_L &\triangleq \|T_L(W_1, W_2) - T_L(W'_1, W'_2)\|_2 \\
&= \left\| \phi(W_1 x_L + W_2 \underbrace{\rho\left(\sum_{j \in C(x_L)} g(T_{L-1,j}(W_1, W_2))\right)}_{\triangleq R(W_1, W_2, x_L)}) \right. \\
&\quad \left. - \phi(W'_1 x_L + W'_2 \rho\left(\sum_{j \in C(x_L)} g(T_{L-1,j}(W'_1, W'_2))\right)) \right\|_2 \\
&\leq C_\phi \|(W_1 - W'_1)x_L\|_2 \\
&\quad + C_\phi \|W_2 R(W_1, W_2, x_L) - W'_2 R(W'_1, W'_2, x_L)\|_2.
\end{aligned} \tag{7}$$

Therefore, in order to find an upper bound for Δ_L , we will bound the two terms in the last inequality separately. We first bound the second term using the sum of $\|W_2 R(W_1, W_2, x_L) - W'_2 R(W_1, W_2, x_L)\|_2$ and $\|W'_2 R(W_1, W_2, x_L) - W'_2 R(W'_1, W'_2, x_L)\|_2$. Note that

$$\begin{aligned}
&\|W'_2 R(W_1, W_2, x_L) - W'_2 R(W'_1, W'_2, x_L)\|_2 \\
&\leq \|W'_2\|_2 \|R(W_1, W_2, x_L) - R(W'_1, W'_2, x_L)\|_2.
\end{aligned} \tag{8}$$

Since g is C_g -Lipschitz, the branching factor of tree is d , and ρ is C_ρ -Lipschitz, therefore, R is dC_gC_ρ -Lipschitz. We will use this fact to bound (8). Specifically,

$$\begin{aligned}
&\|R(W_1, W_2, x_L) - R(W'_1, W'_2, x_L)\|_2 \\
&\leq C_\rho \left\| \sum_{j \in C(x_L)} \left(g(T_{L-1,j}(W_1, W_2)) - g(T_{L-1,j}(W'_1, W'_2)) \right) \right\|_2 \\
&\leq C_\rho \sum_{j \in C(x_L)} \left\| \left(g(T_{L-1,j}(W_1, W_2)) - g(T_{L-1,j}(W'_1, W'_2)) \right) \right\|_2 \\
&\leq C_\rho C_g \sum_{j \in C(x_L)} \|T_{L-1,j}(W_1, W_2) - T_{L-1,j}(W'_1, W'_2)\|_2 \\
&= C_\rho C_g \sum_{j \in C(x_L)} \Delta_{L-1,j}.
\end{aligned}$$

Using this with $\|W'_2\|_2 \leq B_2$ in (8), we immediately get

$$\begin{aligned}
&\|W'_2 R(W_1, W_2, x_L) - W'_2 R(W'_1, W'_2, x_L)\|_2 \\
&\leq B_2 C_\rho C_g \sum_{j \in C(x_L)} \Delta_{L-1,j} \\
&\leq B_2 C_\rho C_g d \max_{j \in C(x_L)} \Delta_{L-1,j}.
\end{aligned}$$

In other words, we bound the effect on each subtree of the root by the maximum effect across these subtrees. Combining this with $\|x_L\|_2 \leq B_x$, we note from (7) that

$$\begin{aligned}\Delta_L &\leq C_\phi B_x \|(W_1 - W'_1)\|_2 \\ &\quad + C_\phi B_2 C_\rho C_g d \max_{j \in C(x_L)} \Delta_{L-1,j} \\ &\quad + C_\phi \|(W_2 - W'_2)R(W_1, W_2, x_L)\|_2.\end{aligned}\tag{9}$$

□

Proof of Lemma 3

Proof. Note from (9) that in order for the change in embedding of the root (due to a small change in weights) to be small, we require that the last term in (9) is small. Toward, that goal we bound the norm of permutation-invariant aggregation at the root node. Specifically, we note that

$$\begin{aligned}&\|R(W_1, W_2, x_L)\|_2 \\ &= \left\| \rho\left(\sum_{j \in C(x_L)} g(T_{L-1,j}(W_1, W_2))\right) \right\|_2 \\ &= \left\| \rho\left(\sum_{j \in C(x_L)} g(T_{L-1,j}(W_1, W_2))\right) - \rho(0) \right\|_2 \\ &\leq C_\rho \left\| \sum_{j \in C(x_L)} g(T_{L-1,j}(W_1, W_2)) \right\|_2 \\ &\leq C_\rho \sum_{j \in C(x_L)} \left\| g(T_{L-1,j}(W_1, W_2)) - g(0) \right\|_2 \\ &\leq C_\rho C_g \sum_{j \in C(x_L)} \left\| T_{L-1,j}(W_1, W_2) \right\|_2 \\ &\leq C_\rho C_g d \max_{j \in C(x_L)} \left\| T_{L-1,j}(W_1, W_2) \right\|_2,\end{aligned}\tag{10}$$

where the norm of the embedding produced by children j of the root using weights W_1 and W_2 is given by

$$\begin{aligned}&\left\| T_{L-1,j}(W_1, W_2) \right\|_2 \\ &= \left\| \phi(W_1 x_{L-1,j} + W_2 R(W_1, W_2, x_{L-1,j})) \right\|_2 \\ &= \left\| \phi(W_1 x_{L-1,j} + W_2 R(W_1, W_2, x_{L-1,j})) - \phi(0) \right\|_2 \\ &\leq C_\phi \left\| W_1 x_{L-1,j} + W_2 R(W_1, W_2, x_{L-1,j}) \right\|_2 \\ &\leq C_\phi \left\| W_1 x_{L-1,j} \right\|_2 + C_\phi \left\| W_2 R(W_1, W_2, x_{L-1,j}) \right\|_2 \\ &\leq C_\phi B_1 B_x + C_\phi B_2 \left\| R(W_1, W_2, x_{L-1,j}) \right\|_2.\end{aligned}\tag{11}$$

Also, since $\|\phi(x)\|_\infty \leq b$ for all $x \in \mathbb{R}^r$ (by our assumption), and $\|\phi(x)\|_2 \leq \sqrt{r}\|\phi(x)\|_\infty$, we obtain

$$\left\| T_{L-1,j}(W_1, W_2) \right\|_2 \leq b\sqrt{r}.\tag{12}$$

Combining (10) and (11), we get the recursive relationship

$$\begin{aligned}
& \|R(W_1, W_2, x_L)\|_2 \\
& \leq C_\rho C_g C_\phi B_1 B_x d \\
& + C_\rho C_g C_\phi B_2 d \max_{j \in C(x_L)} \left\| R(W_1, W_2, x_{L-1,j}) \right\|_2 \\
& \leq C_\rho C_g C_\phi B_1 B_x d \sum_{\ell=0}^{L-1} (C_\rho C_g C_\phi B_2 d)^\ell \\
& = C_\rho C_g C_\phi B_1 B_x d \frac{(\mathcal{C}d)^L - 1}{\mathcal{C}d - 1} .
\end{aligned} \tag{13}$$

On the other hand, combining (10) and (11), we get

$$\|R(W_1, W_2, x_L)\|_2 \leq bd C_\rho C_g \sqrt{r} . \tag{14}$$

Taken together, (13) and (14) yield $\|R(W_1, W_2, x_L)\|_2$

$$\leq C_\rho C_g d \min \left\{ b\sqrt{r}, C_\phi B_1 B_x \frac{(\mathcal{C}d)^L - 1}{\mathcal{C}d - 1} \right\} . \tag{15}$$

□

Proof of Lemma 4

Proof. Using the results from Lemma 2 and 3, we will simplify the bound on Δ_L , i.e., the change in embedding due to a change in weights. We will then bound the change in probability (that the tree label is 1) Λ_L in terms of Δ_L , when we change not only the weights from (W_1, W_2) to W'_1, W'_2 but also the local classifier parameters from β to β' (where β and β' are chosen from a bounded norm family). We show these steps below.

Plugging the bound on $\bar{R} \triangleq \|R(W_1, W_2, x_L)\|_2$ from Lemma 3 in Lemma 2, we get

$$\begin{aligned}
\Delta_L & \leq C_\phi B_x \|W_1 - W'_1\|_2 \\
& + \mathcal{C}d \max_{j \in C(x_L)} \Delta_{L-1,j} \\
& + C_\phi \|W_2 - W'_2\|_2 \bar{R} .
\end{aligned}$$

Expanding the recursion, we note that

$$\Delta_L \leq MB_x \|W_1 - W'_1\|_2 + M\bar{R} \|W_2 - W'_2\|_2 , \tag{16}$$

where

$$M = C_\phi \frac{(\mathcal{C}d)^L - 1}{\mathcal{C}d - 1} . \tag{17}$$

Since $\|A\|_2 \leq \|A\|_F$ for every matrix A , we have

$$\Delta_L \leq MB_x \|W_1 - W'_1\|_F + M\bar{R} \|W_2 - W'_2\|_F . \tag{18}$$

Now since sigmoid is 1-Lipschitz, we have

$$\begin{aligned}
\Lambda_L & = |\psi(\beta^\top T_L(W_1, W_2)) - \psi(\beta'^\top T_L(W'_1, W'_2))| \\
& \leq |\beta^\top T_L(W_1, W_2) - \beta'^\top T_L(W_1, W_2)| \\
& + |\beta'^\top T_L(W_1, W_2) - \beta'^\top T_L(W'_1, W'_2)| \\
& \leq \|\beta - \beta'\|_2 \|T_L(W_1, W_2)\|_2 + B_\beta \Delta_L \\
& \leq \|\beta - \beta'\|_2 \underbrace{(C_\phi B_1 B_x + C_\phi B_2 \bar{R})}_Z + B_\beta \Delta_L
\end{aligned} \tag{19}$$

using (11) and (15). □

Proof of Lemma 5

Proof. Building on results from Lemmas 2-4, we will now show that the change in probability Λ_L can be bounded by ϵ , using a covering of size P , where P depends on ϵ . Moreover, we show that $\log P$ grows as $\mathcal{O}\left(\log\left(\frac{1}{\epsilon}\right)\right)$ for sufficiently small values of ϵ . That is, we can ensure Λ_L is small by using a small covering.

We begin by noting that we can find a covering $\mathcal{C}\left(\beta, \frac{\epsilon}{3Z_\ell}, \|\cdot\|_2\right)$ of size

$$\mathcal{N}\left(\beta, \frac{\epsilon}{3Z_\ell}, \|\cdot\|_2\right) \leq \left(1 + \frac{6ZB_\beta}{\epsilon}\right)^r.$$

Thus, for any specified ϵ , we can ensure that Λ_L is at most ϵ by finding matrix coverings $\mathcal{C}\left(W_1, \frac{\epsilon}{3MB_xB_\beta}, \|\cdot\|_F\right)$ and $\mathcal{C}\left(W_2, \frac{\epsilon}{3M\bar{R}B_\beta}, \|\cdot\|_F\right)$. Using Lemma 8 from (Chen et al., 2019a), we obtain the corresponding bounds on their covering number. Specifically,

$$\begin{aligned} \mathcal{N}\left(W_1, \frac{\epsilon}{3MB_xB_\beta}, \|\cdot\|_F\right) &\leq \left(1 + \frac{6MB_xB_\beta B_1\sqrt{r}}{\epsilon}\right)^{r^2}, \\ \mathcal{N}\left(W_2, \frac{\epsilon}{3M\bar{R}B_\beta}, \|\cdot\|_F\right) &\leq \left(1 + \frac{6M\bar{R}B_\beta B_2\sqrt{r}}{\epsilon}\right)^{r^2}. \end{aligned}$$

The product of all the covering numbers is bounded by

$$P = \left(1 + \frac{6B_\beta \max\{Z, M\sqrt{r} \max\{B_xB_1, \bar{R}B_2\}\}}{\epsilon}\right)^{2r^2+r}.$$

Therefore, the class $\mathcal{B}(L, d, r, \beta, B_1, B_2, B_x)$ that maps a tree-structured input to the probability that the corresponding tree label is 1 can be approximated to within ϵ by a covering of size P . Moreover, when

$$\epsilon < 6B_\beta \max\{Z, M\sqrt{r} \max\{B_xB_1, \bar{R}B_2\}\},$$

we obtain that $\log P$ is at most

$$3r^2 \log\left(\frac{12B_\beta \max\{Z, M\sqrt{r} \max\{B_xB_1, \bar{R}B_2\}\}}{\epsilon}\right).$$

□

Proof of Proposition 7

Proof. We are now ready to prove our generalization bound. Specifically, we invoke a specific form of Dudley's entropy integral to bound the empirical Rademacher complexity $\hat{\mathcal{R}}_{\mathcal{T}}(\mathcal{J}_\gamma)$ via our result on covering from Lemma 5, where recall that \mathcal{J}_γ maps each tree-label pair (t, y) to margin loss $\text{loss}_\gamma(-p(f_c(t; \Theta), y))$.

It is straightforward to show that p is 2-Lipschitz in its first argument, and loss_γ is $\frac{1}{\gamma}$ -Lipschitz. Therefore, we can approximate the class \mathcal{I} that maps (t, y) to $p(f_c(t; \Theta), y)$ by finding an $\frac{\epsilon}{2}$ -cover of \mathcal{B} . Now, note that \mathcal{I} takes values in the interval $[-e, e]$, where

$$e = \|u\|_2 \|T_L(W_1, W_2)\|_2 \leq B_\beta Z.$$

Using Lemma A.5. in (Bartlett et al., 2017), we obtain that

$$\hat{\mathcal{R}}_{\mathcal{T}}(\mathcal{I}) \leq \inf_{\alpha > 0} \left(\frac{4\alpha}{\sqrt{m}} + \frac{12}{m} \int_{\alpha}^{2e\sqrt{m}} \sqrt{\log \mathcal{N}(\mathcal{I}, \epsilon, \|\cdot\|)} d\epsilon \right)$$

where, using Lemma 5, we have

$$\begin{aligned}
& \int_{\alpha}^{2e\sqrt{m}} \sqrt{\log \mathcal{N}(\mathcal{I}, \epsilon, \|\cdot\|)} d\epsilon \\
& \leq \int_{\alpha}^{2e\sqrt{m}} \sqrt{\log \mathcal{N}(\mathcal{B}, \frac{\epsilon}{2}, \text{dist}(\cdot, \cdot))} d\epsilon \\
& \leq \int_{\alpha}^{2e\sqrt{m}} \sqrt{\log U} \leq 2e\sqrt{m} \sqrt{\log U} = 2B_{\beta}Z \sqrt{m \log U}
\end{aligned}$$

with dist being the combination of $\|\cdot\|_2$ and $\|\cdot\|_F$ norms used to obtain covering of size P in Lemma 5, and $\log U$ is

$$3r^2 \log \left(\frac{24B_{\beta} \max\{Z, M\sqrt{r} \max\{B_x B_1, \bar{R}B_2\}\}}{\alpha} \right).$$

Setting $\alpha = \sqrt{\frac{1}{m}}$, we immediately get

$$\hat{\mathcal{R}}_{\mathcal{T}}(\mathcal{I}) \leq \frac{4}{m} + \frac{24B_{\beta}Z}{\sqrt{m}} \sqrt{3r^2 \log Q},$$

where

$$Q = 24B_{\beta}\sqrt{m} \max\{Z, M\sqrt{r} \max\{B_x B_1, \bar{R}B_2\}\}.$$

We finally bound the complexity of class $\hat{\mathcal{R}}_{\mathcal{T}}(\mathcal{J}_{\gamma})$ by noting that loss_{γ} is $\frac{1}{\gamma}$ -Lipschitz, and invoking Talagrand's lemma (Mohri et al., 2012):

$$\hat{\mathcal{R}}_{\mathcal{T}}(\mathcal{J}_{\gamma}) \leq \frac{\hat{\mathcal{R}}_{\mathcal{T}}(\mathcal{I})}{\gamma} \leq \frac{4}{\gamma m} + \frac{24rB_{\beta}Z}{\gamma\sqrt{m}} \sqrt{3 \log Q}.$$

□

Proof of Proposition 8

Proof. We first convey some intuition. Suppose $|X| < 8$, and we assign a distinct index $z(x) \in \{1, 2, \dots, 8\}$ to each message $x \in X$. Then, we can map each x to $10^{-z(x)}$, i.e., obtain a decimal expansion which may be viewed as a one-hot vector representation of at most 10 digits. We would reserve a separate block of 10 digits for each port. This would allow us to disentangle the coupling between messages and their corresponding ports. Specifically, since the ports are all distinct, we can *shift* the digits in expansion of x to the right by dividing by 10^p , where p is the port number of x . This allows us to represent each (x, p) pair uniquely.

Formally, since \mathcal{X} is countable, there exists a mapping $Z : \mathcal{X} \mapsto \mathbb{N}$ from $x \in \mathcal{X}$ to natural numbers. Since X has bounded cardinality, we know the existence of some $N \in \mathbb{N}$ such that $|X| < N$ for all X . Define $k = 10^{\lceil \log_{10} N \rceil}$. We define function f in the proposition as $f(x) = k^{-Z(x)}$. We also take function g in proposition to be $g(p) = 10^{-kN(p-1)}$. That is, we express the function h as $h((x_1, p_1), \dots, (x_{|P|}, p_{|P|})) = \sum_{i=1}^{|P|} g(p_i) f(x_i)$. □